ISSN 1027-5495. Functional Materials, 27, No.3 (2020), p. 482-487.
doi:https://doi.org/10.15407/fm27.03.482 © 2020 — STC "Institute for Single Crystals"

Dependence of the properties of GaAs (111)A and $Ga_{1-x}Al_xAs$ (111)A epitaxial layers on the conditions of their growth by organometallic vapor phase epitaxy

***R.Krukovskyi*[1], *K.Smits*[2], *I.Semkiv*[3], *S.Krukovskyi*[1], *I.Saldan*[4], *H.Ilchuk*[3], *O.Kuntyi*[3]**

[1]Scientific Research Company "Electron-Carat", 202 Stryiska St., 79031 Lviv, Ukraine
[2]Istitute of Solid State Physics, University of Latvia, 8 Kengaraga St., 1063 Riga, Latvia
[3]Lviv Polytechnic National University, 12 Bandery St., 79013 Lviv, Ukraine
[4]I.Franko National University of Lviv, 6 Kyryla and Mefodia St., 79005 Lviv, Ukraine

Received March 11, 2020

The studies of GaAs (111)A and $Ga_{1-x}Al_xAs$ (111)A epitaxial layers have been carried out using low-temperature photoluminescence and high-resolution X-ray diffraction. Correlation between the B^V/A^{III} ratio and the photoluminescence intensity of *n*-GaAs:Si layers prepared through OMVPE on a semi-insulating GaAs (111)A substrate is discussed in details. For an epitaxial layer prepared at the B^V/A^{III} ratio of 94, the peak characteristic of a free exciton was found to be separated from a continuous broad edge band and higher carrier mobility was revealed. High-resolution X-ray diffraction measurements of a two-layer epitaxial *n*-GaAs:Si/*p*-$Ga_{1-x}Al_xAs$:Zn heterostructure prepared on a *p*-GaAs (111)A substrate indicates crystallization of structurally perfect epitaxial heterostructures with a mirror-like surface morphology.
Keywords: photoluminescence, carrier mobility.

Залежність властивостей епітаксійних шарів GaAs (111)A та $Ga_{1-x}Al_xAs$ (111)A на їх умови росту методом металоорганічної парофазної епітаксії. *Р.Круковський, К.Смітс, І.Семків, С.Круковський, І.Салдан, Г.Ільчук, О.Кунтий.*

Проведено вивчення епітаксійних шарів GaAs (111)A та $Ga_{1-x}Al_xAs$ (111)A, використовуючи низькотемпературну фотолюмінесценцію і високороздільну рентгенівську дифракцію. Детально обговорено кореляцію між співвідношенням B^V/A^{III} та інтенсивністю фотолюмінесценції для шарів *n*-GaAs:Si, приготовлених шляхом осадження металоорганічних сполук з газової фази на напівізольовану підкладку GaAs (111)A. Для епітаксійного шару, отриманого при співвідношенні B^V/A^{III} рівному 94, встановлено розділення піку, притаманного вільному екситону, від суцільної широкої прикраєвої смуги та більш високу рухливість носіїв заряду. Вимірювання високороздільною рентгенівською дифракцією двошарової гетероструктури *n*-GaAs:Si/*p*-$Ga_{1-x}Al_xAs$:Zn, сформованої на підкладці *p*-GaAs (111)A, вказують на кристалізацію структурно досконалих епітаксійних гетероструктур з дзеркальною морфологією поверхні.

Проведено изучение эпитаксиальных слоев GaAs (111)A и $Ga_{1-x}Al_xAs$ (111)A, используя низкотемпературную фотолюминесценцию и рентгеновскую дифракцию высокого разрешения. Подробно обсуждена корреляция между соотношением B^V/A^{III} и интенсивностью фотолюминесценции для слоев *n*-GaAs:Si, приготовленных путем осаждения металлорганических соединений из газовой фазы на полуизоляционной подложке GaAs (111)A. Для эпитаксиального слоя, полученного при соотношении B^V/A^{III} равном 94, обнаружено разделение пика, свойственного свободному экситону, от сплошной широкой прикраевой полосы и более высокую подвижность носителей заряда. Измерения рентгеновской дифракцией высокого разрешения двухслойной гетероструктуры *n*-GaAs:Si/*p*-$Ga_{1-x}Al_xAs$:Zn, сформированной на подложке *p*-GaAs (111)A, указывают на кристаллизацию структурно совершенных эпитаксиальных гетероструктур с зеркальной морфологией поверхности.

1. Introduction

Most of the modern high-voltage ultra-high frequency (UHF) transistors manufactured on the basis of GaAs, SiC or GaN using a high electron mobility transistor (HEMT) technology are characterized by a reverse-voltage value not higher than 300 V [1–3]. GaAs is effective, in particular, in improving the efficiency of solar panels and meets modern requirements for energy electronics in industry, production of renewable energy sources or fully electric/hybrid vehicles [4–8]. In the last decade, this has generated interest in the properties of GaAs films [6, 9, 10], as well as GaAs/AlGaAs layers [11–13], depending on the conditions of their synthesis and physico-chemical treatment. Today, the technology of GaAs high-voltage diodes and transistors is very well developed, and the reverse voltage can reach 1700 V [14]. One of the features of the manufacture of such devices is a two-stage technology. At the first stage, a *p-i* region within the range of 40–60 microns is formed by Liquid Phase Epitaxy (LPE). The high reverse voltage value is provided by an *i*-layer a few microns thick, where the hetero-emitter can be obtained by organometallic vapor-phase epitaxy (OMVPE) in the second stage.

It is well-known that the most structurally perfect *i*-layer of GaAs is formed with a (111) crystallographic orientation [3]. However, in practice it is very difficult to form a submicron (111) layer with a high-quality surface morphology [15, 16]. The deposition of a GaAs layer with a crystallographic orientation of (100) is more common and not difficult from the technical point of view. However, special attention is paid to the (111) A/B crystallographic plane, because due to this epitaxial growth, devices with remarkable electrical and physical properties can be produced. The first successful approaches to the process of layer deposition on the Ga-terminated or A face of GaAs (111) substrate were made in [16–18]. Detailed studies of the layer deposition mechanism and its morphology made it possible to prepare a schematic diagram of the correlation between the growth temperature and the arsine partial pressure [17]. Indeed, a mirror-like surface of the layers deposited by OMVPE was obtained within a narrow region of temperatures and total pressure. Depending on the temperature and total pressure in the gas phase, partial decomposition of the A^{III} source (trimethyl Al/Ga/In $\rightarrow$ monomethyl Al/Ga/In) can take place. Similar transformation for B^V source ($AsH_3 \rightarrow {}^*AsH$) is also possible; however, this only occurs on the catalytic surface. Theoretically, the final reaction of the epitaxial growth can be written down as follows:

$$\mathrm{sup{*}Ga(CH_3) + sup{*}AsH \rightarrow GaAs + CH_4}. \quad (1)$$

It was postulated that in the growing process, the main rate-limited stage is the surface reaction between main intermediates $Ga(CH_3)$ and $^*AsH$. Furthermore, the fractional coating of $^*AsH$ active species on the clean GaAs (111)A surface was considered a factor responsible for the surface morphology. As a result, high-quality structures with quantum wells GaAs or $Ga_{1-x}Al_xAs$ on GaAs [17] and GaAs on $Ga_{1-x}Al_xAs$ [16, 18] were obtained in practice. A technological approach to the formation of the *n*-GaAs:Si/*p*-$Ga_{1-x}Al_xAs$:Zn/p^+–GaAs:Zn heterostructure was proposed in [19]. Using the OMVPE method, a submicron layer was synthesized and the doping control was quite easy to accomplish. The main problem to prepare a mirror-like surface was successfully solved due to optimization of the process conditions and B^V/A^{III} ratio, though photoluminescent and structural properties of these epitaxial layers were not sufficiently studied. This paper presents additional

studies of GaAs (111)A and $Ga_{1-x}Al_xAs$ (111)A epitaxial layers using low-temperature photoluminescence (PL) and high-resolution X-ray diffraction (XRD).

2. Experimental

Semi-insulating (s.i.) GaAs (111)A (±0.1°) substrates were received from Wafer Technology LTD, UK. The substrates with thickness of ~ 350±25 microns and resistance of ~ $1\cdot10^{-7}$ Ω/cm did not need a surface treatment since they were ready for OMVPE. Trimethylgallium (Rohm and Haas Electronic materials, USA) was used as an A^{III} source while arsine (Matheson Gas, USA) was used as a B^V source. The effective flow of trimethylgallium was stable and amounted to ~ 36 and ~ 16 sccm, respectively. Disilan (Si_2H_6 200 ppm in H_2; Linde AG, Germany) was used as a donor dopant with an effective flow (Q_{eff}) in the range of ~ 3.6–$4.2\cdot10^{-4}$ sccm. The OMVPE layer deposition process was carried out using a DISCOVERY 180LDM instrument [17].

The carrier mobility was measured using the EMF Hall effect NMS3000 (USA) in van der Pauw geometry. A permanent magnet with a magnetic flux density of 2 000 Gs and a constant-current source with a current in the range of 10 μA to 100 mA were used. Epitaxial layers were prepared on the s.i. substrate with resistivity of 10^7 Ω·cm. The current through the epitaxial layers was 1 nA. The voltage in the range of 1–1.000 μV was controlled by a voltmeter with high input impedance.

Low-temperature PL measurements were carried out at 8 K using an Ar laser with a wavelength of 514.5 nm. The excitation power was approximately ≈30 W/cm^2.

High resolution XRD was used to assess the crystal quality of the prepared epitaxial layers. The structural parameters were calculated based on the initial data obtained with an X'Pert PRO MRD XL diffractometer in a single crystal mode. The diffraction peaks with *hkl* indices of 111, 222 and 333 were used for the structural analysis. The FWHM values of the Bragg peaks were calculated perpendicular and parallel to the diffraction vector using an omega scan.

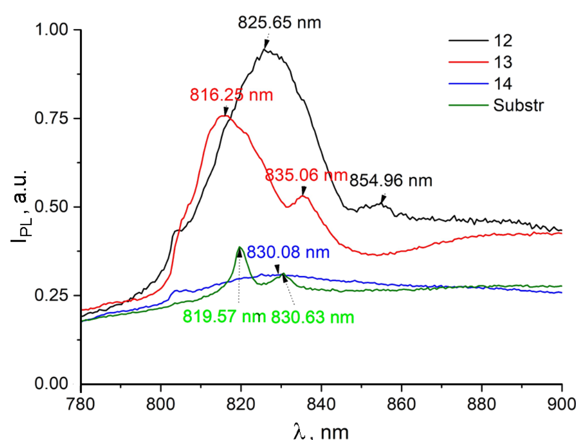

Fig. 1. The low-temperature PL spectra of single n-GaAs:Si layers prepared by OMVPE on a s.i.-GaAs (111)A substrate, together with the spectrum of a clean substrate.

3. Results and discussion

To ensure good surface morphology and high electrical properties of the single *n*-GaAs:Si layer prepared through OMVPE on the GaAs (111)A substrate, the B^V/A^{III} ratio, reaction conditions and technological regime were optimized [19]. The carrier mobility of the epitaxial layers along with OMVPE process conditions are summarized in the Table.

Low-temperature PL spectra of single *n*-GaAs:Si layers, obtained using OMVPE on a GaAs (111) substrate, together with the data on a clean substrate, are shown in Fig. 1. Comparison of samples 12 and 13 reveals complexity of the near-edge band with maxima, respectively, at 816.25 and 825.65 nm. The maximum value for sample 12 corresponds to an exciton associated with a neutral acceptor [20]; while for sample 13, it corresponds to a free exciton [21].

Table. OMVPE process conditions and electrical properties of *n*-GaAs:Si layers

Sample number	Epitaxial layers	B^V/A^{III} ratio	Q_{eff} (Si_2H_6), sccm	$T_{substrate}$, °C	μ_{300K}, cm^2/V·s	N, cm^{-3}	Substrate crystallographic orientation
12	*n*-GaAs:Si	84	$3.6\cdot10^{-4}$	650–680	3050	$7.10\cdot10^{17}$	(111)A
13	*n*-GaAs:Si	94	$3.6\cdot10^{-4}$	650–680	3800	$7.16\cdot10^{17}$	(111)A
14	*n*-GaAs:Si	157	$4.2\cdot10^{-4}$	650–680	2200	$1.10\cdot10^{18}$	(111)A
Substrate	*s.i.*-GaAs	–	–	–		$7.80\cdot10^{14}$	(111)A

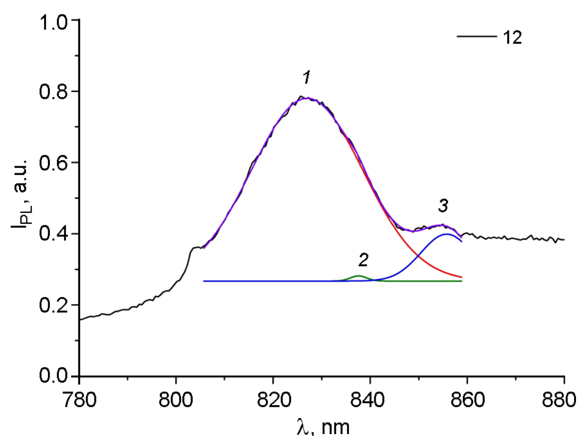

Fig. 2. Deconvolution of a low-temperature PL spectrum for sample 12.

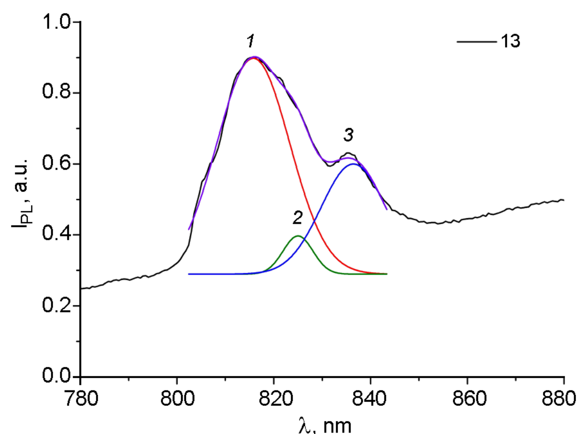

Fig. 3. Deconvolution of a low-temperature PL spectrum for sample 13.

The shoulder on the right side at 854.96 nm for sample 12 can be explained as a donor-acceptor (D-A) junction where the acceptor is represented by silicon atoms located mainly in the interstitial places. A similar band for sample 13 at 835.06 nm might correspond to the band-acceptor (e-A) junction where the acceptor is represented by silicon atoms located in the arsenic sublattice (Si_{As}). There is no intense band for sample 14 though the maximum of its PL spectra might be found around the near-edge band. The low temperature PL spectra of a clean substrate are characterized by two low intensity bands. The first band with a maximum at 819.57 nm corresponds to the transfer caused by the fundamental and excited state of a free exciton and the second band at 830.63 nm — to the e-A junction where the acceptor is represented by silicon atoms.

The shape of the edge bands for samples 12 and 13 is characterized by asymmetry, which confirms that they consist of several peaks. Therefore, the low temperature PL spectra were chosen for deconvolution using the Gaussian function. The deconvolution has helped to understand the nature of the PL spectra for all the samples (Figs. 2–4). Three peaks for sample 12 were obtained at 827.00, 837.60 and 855.76 nm (peak 1, 2 and 3, respectively, Fig. 2). In this case, the mean square deviation (R^2) between experimental and theoretical graphs was 0.99. A similar situation was observed for sample 13 where peaks at 815.77, 825.00 and 836.45 nm were calculated with R^2 value of 0.99 (Fig. 3). Only two peaks at 825.58 and 856.79 nm were found for the PL spectrum of sample 14 with a calculated R^2 value of 0.98 (Fig. 4). The significant blurring of the PL spectrum made it impossible to distinguish between these two peaks, which have a low intensity compared to those in Fig. 2 and 3. A detailed analysis of the deconvolution results indicates the presence of a near-edge band with a maximum in the range of 816–827 nm where there is a significant contribution of the free exciton. The intensity of the near-edge band for sample 14 is much less than those for sample 12 and 13. For all the samples, the deconvolution confirms the bands caused by D-A junctions where an acceptor is represented by silicon atoms. Sample 12 has two bands that might correspond to the D-A junction at 837.60 and 855.76 nm, where the short-wavelength band determines the transfer with acceptor silicon while the long-wave band — with acceptor silicon or germanium [21]. Since only silicon was used as the dopant, it is assumed that these D-A junctions were possible with silicon as an acceptor. For sample 13, the band at 836.45 nm might be caused by the D-A junction, where the donor is represented by

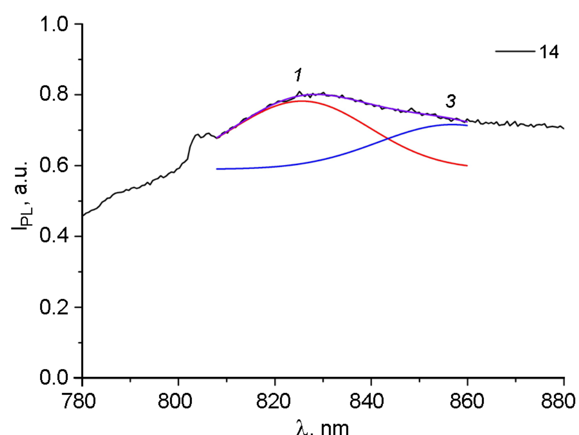

Fig. 4. Deconvolution of a low-temperature PL spectrum for sample 14.

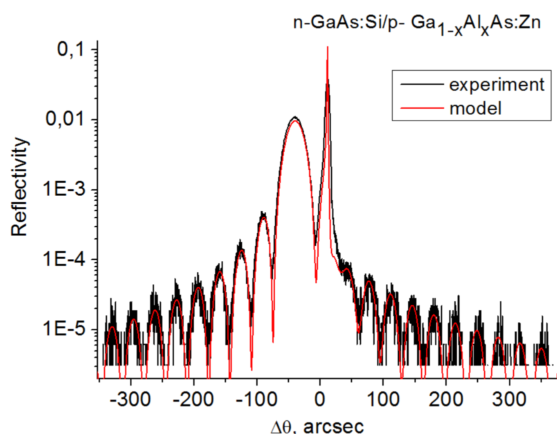

Fig. 5. High-resolution XRD Omega scans of a two layer epitaxial p-GaAs/n-GaAs:Si/p-$Ga_{1-x}Al_xAs$:Zn hetero-structure (experimental in black and modelling in red).

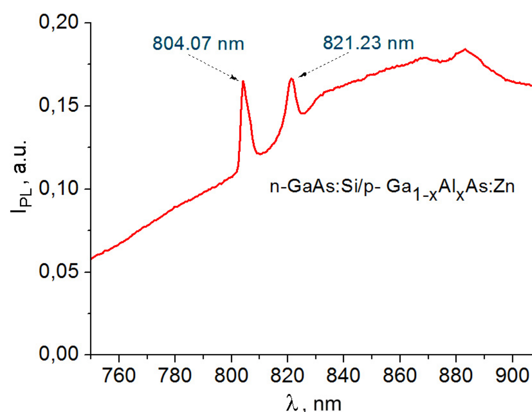

Fig. 6. The low-temperature PL spectra of a two layer epitaxial p-GaAs/n-GaAs:Si/p-$Ga_{1-x}Al_xAs$:Zn hetero-structure.

silicon atoms located in the gallium sublattice (Si_{Ga}), while the acceptor is represented by silicon atoms located in the arsenic sublattice (Si_{As}) [21]. The deconvolution of the PL spectrum for sample 14 shows the short-wavelength band at 856.79 nm that can be explained by the D-A junction with silicon atoms as the acceptor (Fig. 4). Interpretation of the band with a maximum at 825.58 nm is impossible because its full width at half maximum is too large. This is most likely due to point defects of a different nature.

Taking into account the results of experiments on carrier mobility and low-temperature PL, one can determine their dependence on the conditions of the OMVPE process. Sample 13 was prepared at a higher B^V/A^{III} ratio than that for sample 12 (see Table). Under these conditions, the concentration of arsenic vacancies in the epitaxial layer decreases, which leads to a kind of splitting of the continuous PL band into two low-intensity bands with maxima at 816.25 and 835.06 nm (Fig. 1). A lower concentration of arsenic vacancies results in a decrease in the number of silicon atoms that can occupy the positions of arsenic atoms to form Si_{As}-type defects. Most likely, a significant excess of arsenic atoms in the gas phase causes an increase in the total number of point and complex defects; therefore, a low-intensity band at 816.25 nm may appear in sample 13, which corresponds to a free exciton. A further increase in the B^V/A^{III} ratio to 157 in sample 14 (see Table) leads to almost complete disappearance of the near-edge band at about 825–827 nm, and only the peak at 856.79 nm, caused by the D-A junction with silicon atoms as the acceptor can remain (Fig. 4). The complete fading of the near-edge band indicates the deterioration of the PL of epitaxial layers, though their surface morphology is significantly improved [19]. The low-temperature PL spectrum for the *s.i.*-GaAs (111)A substrate (Fig. 1) with a perfect structure shows a narrow near-edge band at 819.57 nm and another band at 830.63 nm inherent in the band of acceptor junctions where the acceptor is represented by background carbon. Because of reduced concentration of charge carriers in pure substrate the intensity of these bands is very low.

However, recent results [19] have confirmed that with the B^V/A^{III} ratio of 157, there can be an optimal value at which the mirror-like morphology is still present; therefore, the structural properties of the GaAs (111)A epitaxial layers do not deteriorate. A strong confirmation of that can be obtained from high-resolution XRD measurements of the two-layer epitaxial p-GaAs(111A)/n-GaAs:Si/p-$Ga_{1-x}Al_xAs$:Zn hetero-structure [21, 22]. The p-GaAs substrate surface has an ideal structure with almost theoretical FWHM value of the reflection line. The two-layer epitaxial structure also has high structural perfection, despite the presence of an interface boundary between n-GaAs:Si and p-$Ga_{1-x}Al_xAs$:Zn layers (Fig. 5). The calculated thickness of the epitaxial layer is 0.485 micron and the composition of $Ga_{1-x}Al_xAs$ solid solution corresponds to $x = 0.30$. The curve resulting from the XRD data is shown in black while that of simulation — in red. The presence of intensity oscillations indicates the high quality of the epitaxial layer, as well as the clarity of the interface boundary between

the substrate and the epitaxial layer. The distances between these oscillations can be used to determine the thickness of the epitaxial heterolayer.

The obtained XRD results are also in agreement with those of low temperature PL (Fig. 6). Using PL experimental data, the calculated composition of $Ga_{1-x}Al_xAs$ solid solution corresponds to x value of 0.28. The PL spectra of the two-layer epitaxial n-GaAs:Si/p-$Ga_{1-x}Al_xAs$:Zn heterostructure prepared on the p-GaAs (111)A substrate consist of two peaks. The first peak at 804 nm is the near-edge line of the $Ga_{1-x}Al_xAs$ solid solution while the second one at 821 nm is the near-edge line of the GaAs layer. A low FWHM value of these PL peaks indicates structural perfection of these epitaxial layers and absence of structural defects on the interface boundary between them. Low intensity of the near-edge line of the $Ga_{1-x}Al_xAs$ solid solution in the PL spectra is predetermined with the deterioration of the photoluminescent properties closer to the transition point from III–V direct to indirect band gap semiconductor at $x > 0.35$ in $Ga_{1-x}Al_xAs$.

4. Conclusions

Based on the experimental results for low-temperature PL, carrier mobility and OMVPE process conditions, the following conclusions can be drawn. An increase in the B^V/A^{III} ratio from 84 to 94 for n-GaAs:Si layers prepared through OMVPE on the *s.i.*-GaAs (111)A substrate results in high-intensity PL spectra, while at the B^V/A^{III} ratio of 157, they degrade. Separation of the peak inherent in a free exciton from a continuous wide-edge band and higher carrier mobility were found for the epitaxial layer obtained at a B^V/A^{III} ratio of 94. High-resolution XRD measurements of a two-layer epitaxial n-GaAs:Si/p-$Ga_{1-x}Al_xAs$:Zn heterostructure prepared on a p-GaAs (111)A substrate indicate crystallization of structurally perfect epitaxial heterostructures with a mirror-like surface morphology.

References

1. T.J.Anderson, M.J.Tadjer, M.A.Mastro et al., *J. Electron. Mater.*, **39**, 478 (2010).
2. M.Tapajna, M.Jurkovic, L.Valik et al., *Appl. Phys. Lett.*, **102**, 243509 (2013).
3. Y.Chii, L.Ganesh, S.Samudra, Power Microelectronics: Device and Process Technologies World Scientific Publishing Company (2008),
4. A.Talhi, A.Belghachi, H.Moughli et al., *Digest J. Nanomater. Biostruct.*, **11**, 1361 (2016).
5. K.Attari, L.Amhaimar, A.Elyaakoubi et al., *Int. J. Photoenergy*, ID 8269358 (2017).
6. R.Alcotte, M.Martin, J.Moeyaert et al., *APL Mater.*, **4**, 046101 (2016).
7. M.Soylu, *Appl. Opt.*, **57**, 6788 (2018).
8. J.Lu, Z.-Q.Fan, J.Gong, X.-W.Jiang, *AIP Adv.*, **7**, 065302 (2017).
9. I.V.Levchenko, V.M.Tomashyk, I.B.Stratiychuk et al., *Functional Materials*, **25**, 165 (2018).
10. S.Torres- Jaramillo, C.Pulzara-Mora, R.Bernal-Correa et al., *Univ. Sci.*, **24**, 523 (2019).
11. H.Jani, L.Chen, L.Duan, *IEEE J. Quant. Electron.*, **56**, 4000208 (2020).
12. M.R.Aziziyan, H.Sharma, J.J.Dubowski, *ACS Appl. Mater. Interfaces*, **11**, 17968 (2019).
13. M.A.Islam, W.M.Hassen, A.F.Tayabali, J.J.Dubowski, *Biochem. Engineer. J.*, **154**, 10743515 (2020).
14. https://powerpulse.net/high-voltage-gaas-power-diode-production-begins-in-dresden/
15. S.Fuek, M.Umemura, N.Yamada et al., *J. Appl. Phys.*, **68**, 97 (1990).
16. E.Mao, S.A.Dickey, A.Majerfeld, et al., *Microelectron. J.*, **28**, 727 (1997).
17. M.Umenura, K.Kuvahara, S.Fuke, *J. App. Phys.*, **72**, 313 (1992).
18. S.Cho, A.Sanz-Hervas, J.Kim et al., *Microelectron. J*, **30**, 455 (1999).
19. S.Larkin, A.Avksentyev, M.Vakiv et al., *Phys. Scripta*, **90**, 094001 (2015).
20. L.Pavesi, M.Guzzi, *J. Appl. Phys.*, **75**, 4779 (1994).
21. V.I.Havrylenko, A.M.Hrekhov, D.V.Korbutiak, V.H.Lytovchenko, Optical Properties of Semiconductors, Naukova Dumka, Kyiv (1987),
22. S.Krukovskyi, H.Ilchuk, R.Krukovskyi et al., *J. Nano Electr. Phys.*, **10**, 03025 (2018).